

Cosmology with Strong Lensing Systems

Shuo Cao

Department of Astronomy, Beijing Normal University, Beijing 100875, China

Marek Biesiada

*Department of Astronomy, Beijing Normal University, Beijing 100875, China;
Department of Astrophysics and Cosmology, Institute of Physics, University of Silesia,
Uniwersytecka 4, 40-007, Katowice, Poland*

Raphaël Gavazzi

*Institute d'Astrophysique de Paris, UMR7095 CNRS - Université Pierre et Marie Curie, 98bis bd
Arago, 75014 Paris, France*

Aleksandra Piórkowska

*Department of Astrophysics and Cosmology, Institute of Physics, University of Silesia,
Uniwersytecka 4, 40-007, Katowice, Poland*

and

Zong-Hong Zhu

Department of Astronomy, Beijing Normal University, Beijing 100875, China

zhuzh@bnu.edu.cn

ABSTRACT

In this paper, we assemble a catalog of 118 strong gravitational lensing systems from SLACS, BELLS, LSD and SL2S surveys and use them to constrain the cosmic equation of state. In particular we consider two cases of dark energy phenomenology: Λ CDM model where dark energy is modeled by a fluid with constant w equation of state parameter and in Chevalier - Polarski - Linder (CPL) parametrization where w is allowed to evolve with redshift: $w(z) = w_0 + w_1 \frac{z}{1+z}$. We assume spherically symmetric mass distribution in lensing galaxies, but relax the rigid assumption of SIS model in favor to more general power-law index γ , also allowing it to evolve with redshifts $\gamma(z)$. Our results for the Λ CDM cosmology show the agreement with values (concerning both w and γ parameters) obtained by other authors. We go further and constrain the CPL parameters jointly with $\gamma(z)$. The resulting confidence regions for the parameters are much better than those obtained with a similar method in the past. They are also showing

a trend of being complementary to the supernova Ia data. Our analysis demonstrates that strong gravitational lensing systems can be used to probe cosmological parameters like the cosmic equation of state for dark energy. Moreover, they have a potential to judge whether the cosmic equation of state evolved with time or not.

Subject headings: gravitational lensing — dark energy — galaxies: fundamental parameters

1. Introduction

Significance of strong gravitational lensing in cosmology has been recognized quite early. Seminal work of Refsdal (1964) demonstrating possibilities of independent determination of the Hubble constant from time delays between images gave momentum to the development of strong gravitational lensing theory. However, it has only recently been possible to determine the Hubble constant from lensing time delays with the precision competitive with other techniques (Suyu et al. 2010). Currently, however, goals and performance of cosmology go far beyond “the quest for two numbers” (H_0 and q_0 – the deceleration parameter). With discovery of the accelerating expansion of the Universe (Riess et al. 1998; Perlmutter et al. 1999), understanding this phenomenon has become one of the most important issues of modern cosmology. Because there is still no fully convincing hints from the side of the theory, we are left with a pragmatic approach to model this phenomenon as the so called dark energy — hypothetical homogeneous fluid phenomenologically described by the barotropic equation of state $p = w\rho$. This approach provides a particularly suitable link between theory and observations. Namely, it encompasses the case of cosmological constant Λ ($w = -1$) and that of the scalar field. If the scalar field settled in an attractor (Ratra & Peebles 1988), w can now be constant (with the fundamental demand that $w < -1/3$ in order to get the acceleration) — this is the so-called XCDM cosmology. It contains Λ CDM as its special case and indeed all constraints on w obtained up to now within XCDM cosmology gave w very close to -1 . Therefore now there is no debate whether the Universe is accelerating, but rather whether w coefficient evolved in time in quite recent epochs (say at $z = 1 - 6$). It is a reasonable question because – as lucidly remarked by Linder – if the scalar field stands behind accelerating expansion, it should have evolved since the only other case of the scalar field we know (the inflaton) clearly evolved because the inflation ended. A very convenient parametrization of $w(z)$ has been proposed by Chevalier & Polarski (2001); Linder (2003): $w(z) = w_0 + w_1 \frac{z}{1+z}$, which is essentially the first-order (linear) Taylor expansion in the scale factor – the true gravitational degree of freedom in FRW cosmology. We will denote this case as CPL thereafter. The problem is that if we use all conventional cosmological probes like SNIa, BAO or CMBR acoustic peaks, we are facing the degeneracy (colinearity) between w_0 and w_1 parameters (stemming from the fact that $w(z)$ overall should be negative). Standard rulers (like BAO and CMBR) and standard candles (SNIa) when used to constrain Ω_m and w parameters acted complementarily in the sense that their respective confidence regions in (Ω_m, w) plane were almost orthogonal. No such complementarity has been proposed so far for w_0, w_1 parameters, although

it has been noticed by Linder (2004) that strong lensing systems are promising in this respect. It is one of the most important reasons motivating our work. Earlier attempts to use strong lensing systems for constraining parameters of the cosmological model were based on two approaches. First was the statistical one based on comparison between empirical distribution of image separations in observed samples of lenses and the theoretical one — using CLASS (Chae et al. 2002), or SQLS samples (Oguri et al. 2012) respectively. Second approach made use of galaxy clusters in the role of lenses (Paczynski & Górski 1981; Sereno 2002; Meneghetti et al. 2005; Gilmore & Natarayan 2009; Jullo et al. 2010) where a single lens (cluster) typically generates ca. 100 images of ca. 30-40 different sources (distant galaxies).

We use another method which can be traced back to the papers of e.g. Futamase & Yoshida (2001); Biesiada (2006); Grillo et al. (2008). However, similarly as with the Hubble constant, it is only quite recently when reasonable catalogs of strong lenses: containing more than 100 lenses, with spectroscopic as well as astrometric data, obtained with well defined selection criteria are becoming available. It is also only recently when our knowledge about structure and evolution of early type galaxies allows us to undertake the assessment of such important factor as mass density profile. Recent works (Biesiada, Piórkowska, & Malec 2010; Cao et al. 2012) provided first successful applications of the proposed method in the context of dark energy, although small samples have not allowed for stringent constraints. This encourages us to improve and develop it further. On a new sample of 118 lenses compiled from SLACS, BELLS, LSD and SL2S surveys we constrain the cosmic equation of state in Λ CDM cosmology and in CPL parametrization. Moreover we relax the rigid assumption of SIS model to general power-law density profile allowing the power-law index to evolve with redshifts.

This paper is organized as follows. In Section 2, we briefly describe the methodology. Then, in Section 3 we introduce the strong lensing data used in our analysis. The results are presented in Section 4 and concluded in Section 5.

2. Methodology

As one of the successful predictions of General Relativity in the past decades, strong gravitational lensing has become a very important astrophysical tool allowing us to use individual lensing galaxies to measure cosmological parameters (Treu et al. 2006; Grillo et al. 2008; Biesiada, Piórkowska, & Malec 2010; Cao et al. 2012). For a specific strong lensing system with the intervening galaxy acting as a lens, the multiple image separation of the source depends only on angular diameter distances to the lens and to the source, as long as one has a reliable model for the mass distribution within the lens.

Moreover, compared with late-type and unknown-type counterparts, early-type galaxies (ETGs, ellipticals) are more likely to serve as intervening lenses for the background sources (quasars or galaxies). This is because such galaxies contain most of the cosmic stellar mass of the Universe.

This property affects statistics of gravitational lensing phenomenon which leads to a sample dominated by early-type galaxies (see Kochanek et al. (2000) and references therein). Here, we encounter a critical issue that still needs to be addressed in a systematic way: such properties of early-type galaxies like their formation and evolution are still not fully understood. Fortunately, a sample of well-defined strong lensing systems is now available and can be used to study the mass density distribution in early-type galaxies.

In principle, the lens model often fitted to the observed images is based on a singular isothermal ellipsoid (SIE) model, in which the projected mass distribution is elliptical (Ratnatunga et al. 1999). In this paper, we will take a simpler approach and assume spherical symmetry. For a moment we will refer to the singular isothermal sphere (SIS) model instead which will then be generalized.

The main idea of our method is that formula for the Einstein radius in a SIS lens

$$\theta_E = 4\pi \frac{\sigma_{SIS}^2}{c^2} \frac{D_{ls}}{D_s} \quad (1)$$

depends on the cosmological model through the ratio of (angular-diameter) distances between lens and source and between observer and lens. The angular diameter distance in flat Friedmann-Robertson-Walker cosmology reads

$$D(z; \mathbf{p}) = \frac{1}{1+z} \frac{c}{H_0} \int_0^z \frac{dz'}{h(z'; \mathbf{p})} \quad (2)$$

where H_0 is the present value of the Hubble function and $h(z; \mathbf{p})$ is a dimensionless expansion rate dependent on redshift z and cosmological model parameters are: $\mathbf{p} = \{\Omega_m, w\}$ for Λ CDM cosmology or $\mathbf{p} = \{\Omega_m, w_0, w_1\}$ for the CPL parametrization of evolving equation of state. More specifically, $h^2(z; \mathbf{p}) = \Omega_m(1+z)^3 + (1-\Omega_m)(1+z)^{3(1+w)}$ for Λ CDM cosmology and $h^2(z; \mathbf{p}) = \Omega_m(1+z)^3 + (1-\Omega_m)(1+z)^{3(1+w_0+w_1z)} \exp(-\frac{3w_1z}{1+z})$ for CPL parametrization.

Provided one has a reliable knowledge about the lensing system, i.e. the Einstein radius θ_E (from image astrometry) and stellar velocity dispersion σ_{SIS} (from central velocity dispersion σ_0 obtained from spectroscopy), one can use it to test the background cosmology. This method is independent of the Hubble constant value (which gets canceled in the distance ratio) and is not affected by dust absorption or source evolutionary effects. It depends, however, on the reliability of lens modeling (e.g. SIS assumption) and measurements of σ_0 . Hopefully, starting with the Lens Structure and Dynamics (LSD) survey and the more recent SLACS survey, spectroscopic data for central parts of lens galaxies became available allowing to assess their central velocity dispersions. There is a growing evidence for homologous structure of late type galaxies (Koopmans et al. 2006, 2009; Treu et al. 2006) supporting reliability of SIS assumption.

In our method, cosmological model enters not through a distance measure directly, but rather through a distance ratio

$$\mathcal{D}^{th}(z_l, z_s; \mathbf{p}) = \frac{D_{ls}(\mathbf{p})}{D_s(\mathbf{p})} = \frac{\int_{z_l}^{z_s} \frac{dz'}{h(z'; \mathbf{p})}}{\int_0^{z_s} \frac{dz'}{h(z'; \mathbf{p})}} \quad (3)$$

and respective observable counterpart reads

$$\mathcal{D}^{obs} = \frac{c^2 \theta_E}{4\pi \sigma_0^2}$$

From one side this circumstance is a complication, but it also offers an advantage. Namely, as we already mentioned, w_0 and w_1 parameters are intrinsically anti correlated, which makes it difficult to constrain them. In the \mathcal{D} ratio, however a competition between two angular diameter distances may lead to positive correlations between w_0 and w_1 as discussed recently in (Piorkowska et al. 2013). Constraints on cosmological models using this method have been obtained e.g. in Biesiada, Piorkowska, & Malec (2010); Biesiada, Malec & Piorkowska (2011); Cao et al. (2012).

One objection one might rise towards the proposed method is the rigid assumption of the SIS model for the lens. Although there are some arguments that inside Einstein radii total mass density follows isothermal profile (Koopmans et al. 2006), one can expect the deviation from the isothermal profile and its evolution with redshift. The last point theoretically stems from the structure formation theory (ellipticals as a result of mergers) and to some extent has been supported observationally (Ruff et al. 2011; Brownstein et al. 2012; Sonnenfeld et al. 2013b).

Therefore we have to generalize the SIS model to spherically symmetric power-law mass distribution $\rho \sim r^{-\gamma}$. First, we recall that location of observed images, hence the knowledge of θ_E provides us with the mass M_{lens} inside the Einstein radius: $M_{lens} = \pi R_E^2 \Sigma_{cr}$ where: $R_E = \theta_E D_l$ is the physical Einstein radius (in [kpc]) in the lens plane and $\Sigma_{cr} = \frac{c^2}{4\pi G} \frac{D_s}{D_l D_{ls}}$ is the critical projected mass density for lensing (Schneider et al. 1992). Finally we have:

$$M_{lens} = \frac{c^2}{4G} \frac{D_s D_l}{D_{ls}} \theta_E^2 \quad (4)$$

If one has spectroscopic data providing the velocity dispersion σ_{ap} inside the aperture (more precisely, luminosity averaged line-of-sight velocity dispersion), then after solving spherical Jeans equation (assuming that stellar and mass distribution follow the same power-law and anisotropy vanishes) one can assess the dynamical mass inside the aperture projected to lens plane (Koopmans et al. 2005) and scale it to the Einstein radius

$$\begin{aligned} M_{dyn} &= \frac{\pi}{G} \sigma_{ap}^2 R_E \left(\frac{R_E}{R_{ap}} \right)^{2-\gamma} f(\gamma) \\ &= \frac{\pi}{G} \sigma_{ap}^2 D_l \theta_E \left(\frac{\theta_E}{\theta_{ap}} \right)^{2-\gamma} f(\gamma) \end{aligned} \quad (5)$$

where

$$\begin{aligned} f(\gamma) &= -\frac{1}{\sqrt{\pi}} \frac{(5-2\gamma)(1-\gamma)}{3-\gamma} \frac{\Gamma(\gamma-1)}{\Gamma(\gamma-3/2)} \\ &\times \left[\frac{\Gamma(\gamma/2-1/2)}{\Gamma(\gamma/2)} \right]^2 \end{aligned} \quad (6)$$

By combining Eq. (4) and Eq. (5), we obtain

$$\theta_E = 4\pi \frac{\sigma_{ap}^2}{c^2} \frac{D_{ls}}{D_s} \left(\frac{\theta_E}{\theta_{ap}} \right)^{2-\gamma} f(\gamma) \quad (7)$$

Now, our observable is

$$\mathcal{D}^{obs} = \frac{c^2 \theta_E}{4\pi \sigma_{ap}^2} \left(\frac{\theta_{ap}}{\theta_E} \right)^{2-\gamma} f^{-1}(\gamma) \quad (8)$$

and its theoretical counterpart (the distance ratio) $\mathcal{D}^{th}(z_l, z_s; \mathbf{p})$ is given by Eq.(3).

Fractional uncertainty of \mathcal{D} (after calculating all relevant partial derivatives and simplifying terms) is

$$\delta\mathcal{D} = \frac{\Delta\mathcal{D}}{\mathcal{D}} = \sqrt{4(\delta\sigma_{ap})^2 + (1-\gamma)^2(\delta\theta_E)^2} \quad (9)$$

Following the SLACS team we took the fractional uncertainty of the Einstein radius at the level of 5% i.e. $\delta\theta_E = 0.05$ – the same for all lenses.

Theoretically for a single system one could use σ_{ap} , but because we deal with a sample of lenses, we shall also transform all velocity dispersions measured within an aperture to velocity dispersions within circular aperture of radius $R_{eff}/2$ (half the effective radius) following the prescription of Jørgensen et al. (1995a,b): $\sigma_0 = \sigma_{ap}(\theta_{eff}/(2\theta_{ap}))^{-0.04}$. In the literature it has also been denoted as σ_{e2} . We adopt the convention to denote observed angular Einstein radius or effective radius as θ_E or θ_{eff} with the notation R_E or R_{eff} reserved for physical values (in [kpc]) of respective quantities. In our analysis however, we will consider two cases: with σ_{ap} and σ_0 . While using σ_0 , the equations Eq. (7), Eq. (8) and Eq. (9) should be modified by replacing σ_{ap} with σ_0 . In principle (i.e. within the power-law model), the use of σ_{ap} should work because we rescale to the Einstein radius anyway. However, the use of σ_0 makes our observable \mathcal{D}^{obs} more homogeneous for the sample of lenses located at different redshifts. One may worry about additional uncertainties introduced into the error budget this way since the measurement of θ_{eff} bears its own uncertainty. Arguing that fractional uncertainty for the effective radius is at the level of 5% (like for the Einstein radius) and bearing in mind that in the Jørgensen formula θ_{eff} is raised to a very small power one can estimate that uncertainties of the effective radius contribute less than 1% to the uncertainty of σ_0 .

Then using routines available within CosmoMC package (Lewis & Bridle 2002), we performed Monte Carlo simulations of the posterior likelihood $\mathcal{L} \sim \exp(-\chi^2/2)$ where

$$\chi^2 = \sum_{i=1}^{118} \left(\frac{\mathcal{D}^{th}(z_{l,i}, z_{s,i}; \mathbf{p}, \gamma) - \mathcal{D}^{obs}(\sigma_{0,i}, \theta_{E,i})}{\Delta\mathcal{D}_i^{obs}} \right)^2 \quad (10)$$

In our fits mass density power-law index γ was taken as a free parameter fitted together with cosmological parameters \mathbf{p} . It has been suggested by Ruff et al. (2011) and further supported by Brownstein et al. (2012); Sonnenfeld et al. (2013a), that mass density power-law index γ of massive elliptical galaxies evolves with redshift. On a combined sample of lenses from SLACS, SL2S and LSD they fitted the $\gamma(z_l)$ data with the linear relation and obtained $\gamma(z_l) = 2.12_{-0.04}^{+0.03}$ –

$0.25_{-0.12}^{+0.10} \times z_l + 0.17_{-0.02}^{+0.02}(\text{scatter})$. Therefore we also performed fits assuming the linear relation: $\gamma(z_l) = \gamma_0 + \gamma_1 z_l$ treating γ_0 and γ_1 as free parameters together with cosmological ones.

3. Data sets

In order to implement the methodology described in Section 2, we have made a comprehensive compilation of 118 strong lensing systems from four surveys: SLACS, BELLS, LSD and SL2S. The Sloan Lens ACS Survey (SLACS) and the BOSS emission-line lens survey (BELLS) are spectroscopic lens surveys in which candidates are selected respectively from Sloan Digital Sky Survey (SDSS-III) data and Baryon Oscillation Spectroscopic Survey (BOSS). BOSS has been initiated by upgrading SDSS-I optical spectrographs (Eisenstein et al. 2011). The idea was to take the spectra of early type galaxies and to look for the presence of emission lines at redshift higher than that of the target galaxy. Candidates selected this way were followed-up with HST ACS snapshot imaging and after image processing: subtraction of the de Vaucouleurs profile of the target galaxy, those displaying multiple images and/or Einstein rings have been classified as confirmed lenses. For our purpose SLACS data comprising 57 strong lenses were taken after Bolton et al. (2008a) and Auger et al. (2009). And the BELLS data containing 25 lenses were taken from Brownstein et al. (2012).

Lenses Structure and Dynamics (LSD) survey was a predecessor of SLACS in the sense that combined image and lens velocity dispersion data were used to constrain the structure of lensing galaxies. However, it was different, because lenses were selected optically (as multiple images of sources with identified lensing galaxies) and then followed-up spectroscopically. Therefore, in order to comply with SLACS and BELLS, we took only 5 most reliable lenses from LSD: CFRS03.1077; HST 14176+5226; HST 15433+5352 after Treu & Koopmans (2004), Q0047-281 after Koopmans & Treu (2002), and MG2016+112 after Treu & Koopmans (2002).

At last the Strong Lensing Legacy Survey (SL2S) is a project dedicated to finding galaxy-scale lenses in the Canada France Hawaii Telescope Legacy Survey (CFHTLS). The targets are massive red galaxies and an automated **RingFinder** software is looking for tangentially elongated blue features around (Gavazzi et al. 2014). If found they are followed-up with HST and spectroscopy. The data for a total of 31 lenses we include here were taken from Sonnenfeld et al. (2013a,b).

Our sample is presented in Table 1. It contains all relevant data necessary to perform cosmological model fits according to our methodology presented in Section 2. The Einstein radius derivation method is more or less consistent across different surveys considered here. After subtracting de Vaucouleurs profile of the deflector, the Einstein radii were measured by fitting model mass distributions to generate model lensed images and comparing them to the observed images. The mass distribution of the main lenses was modeled as singular isothermal ellipsoids (SIE), while in several systems, an external shear component was also added to describe the lensing effect of nearby groups or clusters. Even though individual uncertainties of this procedure are different

depending on the survey and on whether the image was taken from the Earth or from space (HST) there is a consensus that in average the relative uncertainty of the Einstein radius is at the level of 5%. Apertures for SLACS and BELLS were taken as $1.5''$ and $1''$ respectively according to the source papers. For LSD and SL2S lenses we have assessed the aperture size from the sizes x, y of the slit reported in source papers. The last column gives the velocity dispersion within a half effective radius calculated according to Jørgensen formula. Fig. 1 shows the scatter plot of our lensing systems. One can see that inclusion of the SL2S lenses resulted in a fair coverage of lenses and sources redshifts.

Fig. 2 presents histograms of lens and source redshift with the contribution of respective surveys over-plotted in the same color convention as in Fig. 1. Different surveys have the following median values of the lens redshifts: SLACS – $z_l = 0.215$, BELLS – $z_l = 0.517$, LSD – $z_l = 0.81$ and SL2S – $z_l = 0.456$. The above values refer to lenses used by us. SL2S survey – an ongoing one – is particularly promising for the future since it already reached the maximum lens redshift of $z_l = 0.8$.

4. Results

Although the lens redshift z_l and source redshift z_s both cover a wide range in our sample, distance ratio \mathcal{D} is still confined to a very compact range of values, which leads to poor constraining power for Ω_m parameter (Biesiada, Piórkowska, & Malec 2010). Therefore in this paper, we fix Ω_m at the best-fit value $\Omega_m = 0.315$ based on the recent Planck observations (Ade et al. 2014). This disadvantage of our method, i.e. the necessity of taking a prior for the matter density parameter, is to a certain degree alleviated by the benefit of being independent of the Hubble constant which cancels in the distance ratio. Consequently H_0 and its uncertainty do not influence the results. Performing fits to different cosmological scenarios on the $n = 118$ strong lensing sample, we obtain the results displayed in Table 2. The marginalized probability distribution of each parameter and the marginalized 2D confidence contours are presented in Fig. 3-6.

We started our analysis with dark energy phenomenon modeled by barotropic fluid having constant equation of state coefficient w and we considered two cases of mass density profiles in lenses: a non-evolving power-law density profile and an evolving one (denoted in Table 2 as $XCDM1$ and $XCDM2$, respectively). Power-law exponents γ , γ_0 and γ_1 were treated as free parameters to be fitted.

First, we consider fits on our sample taking the aperture velocity dispersion σ_{ap} as the lens parameter. In the $XCDM$ model where w is the only free cosmological parameter and γ is the mass density power-law index parameter, we obtain $w = -1.45_{-0.95}^{+0.54}$ and $\gamma = 2.03 \pm 0.06$. In the second case, when the power-law mass density profile was allowed to evolve: $\gamma(z_l) = \gamma_0 + \gamma_1 z_l$, the best-fit values for the parameters are $w = -1.48_{-0.94}^{+0.54}$, $\gamma_0 = 2.06 \pm 0.09$, and $\gamma_1 = -0.09 \pm 0.16$. One can see that w coefficient obtained from the strong lensing sample is consistent with the Λ CDM model ($w = -1$) at 1σ level. Fits on the γ parameter also reveal compatibility between our sample

of lenses and the previous smaller combined sample from SLACS, SL2S and LSD (Ruff et al. 2011; Sonnenfeld et al. 2013b). In an attempt to constrain cosmology with the CPL parametrization describing an evolving cosmic equation of state, we first consider the case that both w_0 , w_1 and γ_0 , γ_1 are free parameters (denoted in Table 2 as *CPL1*). By fitting the CPL model to the full $n = 118$ sample with σ_{ap} , we get the marginalized 1σ constraints of the parameters $w_0 = -0.15^{+1.27}_{-1.60}$, $w_1 = -6.95^{+7.25}_{-3.05}$ and $\gamma_0 = 2.08 \pm 0.09$, $\gamma_1 = -0.09 \pm 0.17$. By fixing γ parameters at our best-fit values (denoted in Table 2 as *CPL2*), the best-fit values for the two cosmic equation of state parameters are: $w_0 = -0.16^{+1.21}_{-1.48}$ and $w_1 = -6.25^{+6.25}_{-3.75}$. We also show the marginalized 1σ and 2σ contours of the two parameter in Fig. 6. It can be seen that, comparing to the previous analysis with a smaller sample (Biesiada, Piórkowska, & Malec 2010; Cao et al. 2012), fits for w_0 and w_1 are significantly improved with a larger strong lensing sample.

Working on the sample with the aperture corrected velocity dispersion σ_0 , we find that the dark energy equation of state parameter ($w = -1.15^{+0.56}_{-1.20}$ and $w = -1.35^{+0.67}_{-1.50}$) agrees very well with the respective value derived from Planck observations combined with BAO data ($w = -1.13^{+0.13}_{-0.10}$) (Ade et al. 2014). Constraints on the mass density power-law index parameters ($\gamma_0 = 2.13^{+0.07}_{-0.12}$, $\gamma_1 = -0.09 \pm 0.17$) are even more consistent with the previous analysis (Ruff et al. 2011; Sonnenfeld et al. 2013b) especially with σ_0 taken as the lens parameter. In the case of evolving cosmic equation of state (CPL parametrization), we obtain $w_0 = -1.00^{+1.54}_{-1.95}$, $w_1 = -1.85^{+4.85}_{-6.75}$ and $\gamma_0 = 2.14^{+0.07}_{-0.10}$, $\gamma_1 = -0.10 \pm 0.18$. By fixing γ parameters at the best-fit values, the fits for w_0 and w_1 are: $w_0 = -1.05^{+1.43}_{-1.77}$ and $w_1 = -1.65^{+4.25}_{-6.35}$. One can see fairly good agreement between our results obtained by using distance ratio method for strong lensing systems and the concordance Λ CDM model. In order to compare our fits with the results obtained using supernovae Ia, likelihood contours obtained with the latest Union2.1 compilation (Suzuki et al. 2012) consisting of 580 SN Ia data points are also plotted in Fig. 6. For a fair comparison, the matter density parameter Ω_m is also fixed at the Planck best-fit value $\Omega_m = 0.315$ and the systematic errors of observed distance moduli are also considered in the likelihood calculation (Cao & Zhu 2014). We see that 1σ confidence regions from the two data sets overlap very well with each other. This means that the results obtained on the sample of strong lenses are consistent with the SNIa fits. This consistency at 1σ level is different from earlier results obtained with smaller sample of lenses (Biesiada, Piórkowska, & Malec 2010; Cao et al. 2012).

One can clearly see from Fig 6 that principal axes of confidence regions obtained with supernovae and strong lenses are inclined at higher angles than in previous studies (Biesiada, Piórkowska, & Malec 2010; Biesiada, Malec & Piórkowska 2011; Cao et al. 2012). This sustains the hope that careful choice of the sample in terms of lens and source redshifts, would eventually realize an ultimate dream to have a complementary probe breaking the degeneracy in (w_0, w_1) plane (discussed in Linder (2004); Piórkowska et al. (2013)). This will be a subject of another study.

Our method based on distance ratio for strong gravitational lensing systems may also contribute to testing the consistency between luminosity and angular diameter distances (Cao & Zhu 2011a,b). As it is well known, these two observables are related to each other via Etherington reciprocity

relation. Earlier discussions of this issue can be found in Bassett & Kunz (2004); Uzan et al. (2004); Holanda, Lima & Ribeiro (2010).

In order to study the systematics and scatter in our method we performed the diagnostics of residuals. Plots of relative residuals $(\mathcal{D}^{obs} - \mathcal{D}^{th})/\mathcal{D}^{obs}$ as a function of z_l , z_s , R_E/R_{eff} and σ_0 for the case of Λ CDM cosmology, assuming non-evolving mass density profile in lenses, are displayed in Fig. 7. This figure is representative of similar diagnostics for the CPL case and evolving mass density profile. One can see that there is no correlation between residuals and the redshifts of lenses or sources, as well as with the Einstein radius relative to the effective radius. However, there is a noticeable anti-correlation (correlation coefficient ca. -0.6) with the velocity dispersion. This trend is especially pronounced for lenses with $\sigma_0 < 230$ km/s. If one excluded small velocity dispersion lenses the result would be comparable to other diagnostics discussed. This effect is probably related to recent findings of Shu et al. (2014) who extended SLACS survey into lower mass region and found that elliptical galaxies with smaller observed velocity dispersions are more centrally concentrated. In any case, however there is a considerable scatter left (at the level of $\pm 50\%$). This scatter could be attributable to individual properties of lenses, like their environment or deviation from the spherical symmetry. From theoretical point of view it has been known for a long time (Falco, Gorenstein & Shapiro 1985) that there exists a transformation of mass distribution in the lens that leaves all observables invariant. This is so called “mass-sheet” degeneracy — a topic which has recently revived in the context of double Einstein Ring lenses (Schneider & Sluse 2013). However, from the physical point of view one of the main ingredients of the “mass-sheet” degeneracy comes from the contamination of secondary lenses (clumps of matter along or close to the line of sight). Such factors have not been considered in our methodology and their proper inclusion is still challenging.

5. Conclusions

In conclusion, our analysis demonstrates that strong gravitationally lensed systems can already now be used to probe cosmological parameters, especially the cosmic equation of state for dark energy. One may say that the approach initiated in Biesiada (2006); Grillo et al. (2008); Biesiada, Piórkowska, & Malec (2010); Cao et al. (2012) can be further developed.

However, there are several sources of systematics we do not consider in this paper and which remain to be addressed in the future analysis. Let us start with simplified assumptions underlying our method. The first one is related to the interpretation of observed velocity dispersions. In this paper, we adopted the spherical Jeans equation to connect observed velocity dispersions to the masses and we did it assuming that anisotropy β parameter was zero. As shown in Koopmans et al. (2006) and in more detailed way in Koopmans et al. (2005) (the equations generalizing our Eq. 5-7 to arbitrary β can be found there) anisotropy parameter is degenerated with the slope γ . Therefore in our approach power-law index should be understood as an effective descriptor capturing both the density profile and anisotropy of the velocity dispersions. This effect clearly contributes to the

scatter in our results. Another issue is the three-dimensional shape of lensing galaxies, the prolateness/oblateness of lensing galaxies can systematically bias the connection between the mass and the velocity dispersion (Chae 2003). This effect also contributes to the scatter at high redshifts and might reveal as a systematic effect at low redshifts. All these effects are hard to be rigorously accounted in context of cosmological studies like in this paper. Recent results on this issue can be found in Barnabé, Spiniello & Koopmans (2014).

The other systematic is the influence of the line of sight (foreground and background) contamination. The problem has been recognized long time ago (Kochanek & Apostolakis 1988; Bar-Kana 1996; Keeton, Kochanek & Seljak 1997) with a heuristic suggestion that adding an external shear to an elliptic lens model greatly improves the fits of multiple image configurations. Wambsganss, Bode & Ostriker (2005) addressed the question of secondary lenses on the line of sight and concluded that the role of secondary lenses is a strong function of source redshift and can be important in 38% of cases for a source at $z_s = 3.5$. High redshift sources are advantageous from the point of view of dark energy studies and at the same time they are challenging from the point of view of line of sight contamination. One of the most recent studies (Jaroszyński & Kostrzewa-Rutkowska 2012) trying to quantify the influence of the matter along line of sight on strong lensing used the technique of simulations of many multiple image configurations using a realistic model of light propagation in an inhomogeneous Universe model (based on the Millenium simulation). Further progress in this direction has recently been achieved by Collett et al. (2014) in a paper accompanied with publicly available code `Pangloss`. They used a simple halo model prescription for reconstructing the mass along a line of sight up to intermediate redshifts and calibrated their procedure with ray-tracing through the Millenium Simulation.

Finally, as proposed by Rusin, Kochanek & Keeton (2003), another approach to constrain the power-law index γ of lensing galaxies is to assume a self-similar mass profile and combine different strong lens systems to statistically constrain the mass profile, which could be combined with the method considered in this paper to break the degeneracy between γ and cosmological parameters. Inclusion of this combination into cosmological use of strong lensing systems will be a subject of a separate paper.

Acknowledgements

The authors are grateful to the referee for very useful comments which allowed to improve the paper. This work was supported by the Ministry of Science and Technology National Basic Science Program (Project 973) under Grants Nos. 2012CB821804 and 2014CB845806, the Strategic Priority Research Program “The Emergence of Cosmological Structure” of the Chinese Academy of Sciences (No. XDB09000000), the National Natural Science Foundation of China under Grants Nos. 11373014 and 11073005, the Fundamental Research Funds for the Central Universities and Scientific Research Foundation of Beijing Normal University, and China Postdoctoral Science Foundation under grant No. 2014M550642. R.G. acknowledges support from the CNES.

Part of the research was conducted within the scope of the HECOLS International Associated Laboratory, supported in part by the Polish NCN grant DEC-2013/08/M/ST9/00664 - M.B., A.P., R.G. gratefully acknowledge this support. M.B. obtained approval of foreign talent introducing project in China and gained special fund support of foreign knowledge introducing project. He also gratefully acknowledges hospitality of Beijing Normal University.

REFERENCES

- Ade, P.A.R., et al. [Planck Collaboration] 2014, accepted by A&A
- Auger, M. W., et al. 2009, *ApJ*, 105, 1099
- Aurière, M. 1982, *A&A*, 109, 301
- Bar-Kana, R. 1996, *ApJ*, 468, 17
- Barnabé, M., Spiniello, C., & Koopmans, L.V.E., 2014 “Dissecting the 3D structure of elliptical galaxies with gravitational lensing and stellar kinematics”, in Eds. B.L. Ziegler, F. Combes, H. Dannerbauer, M. Verdugo, “Galaxies in 3D across the Universe”, Proceedings of the IAU Symposium No. 309 [arXiv:1409.4197]
- Bassett, B. A., & Kunz, M. 2004, *PRD*, 69, 101305
- Biesiada, M. 2006, *PRD*, 73, 023006
- Biesiada, M., Piórkowska, A., & Malec, B. 2010, *MNRAS*, 406, 1055
- Biesiada, M., Malec, B., & Piórkowska, A. 2011, *RAA*, 11, 641
- Bolton, A. S., et al. 2008a, *ApJ*, 682, 964
- Brownstein, et al. 2012, *ApJ*, 744, 41
- Canizares, C. R., Grindlay, J. E., Hiltner, W. A., Liller, W., & McClintock, J. E. 1978, *ApJ*, 224, 39
- Cao, S., & Liang, N. 2011a, *RAA*, 11, 1199
- Cao, S., & Zhu, Z.-H. 2011b, *China Series G*, 54, 2260 [arXiv:1102.2750]
- Cao, S., et al. 2012, *JCAP*, 3, 16
- Cao, S., & Zhu, Z.-H. 2014, *PRD*, 90, 083006
- Chae, K.-H., et al. 2002, *PRL*, 89, 151301
- Chae, K.-H. 2003, *MNRAS*, 346, 746

- Chevalier, M., & Polarski, D. 2001, *IJMPD*, 10, 213
- Collett T.E., et al. 2013, *MNRAS*, 432, 679-692 [arXiv:1303.6564]
- Djorgovski, S., & King, I. R. 1984, *ApJL*, 277, L49
- Eisenstein, D. J., et al. 2011, *AJ*, 142, 72 [arXiv:1101.1529]
- Falco, E. E., Gorenstein, M. V., Shapiro, I. I. 1985, *ApJ*, 289, L1
- Futamase, T., & Yoshida, S. 2001, *Prog. Theor. Phys.*, 105, 887
- Gavazzi, R., Marshall, P.J., Treu, T. & Sonnenfeld, A., “RingFinder: automated detection of galaxy-scale gravitational lenses in ground-based multi-filter imaging data”, (2014) *ApJ* accepted [arXiv:1403:1041]
- Gilmore, J., & Natarayan, P. 2009, *MNRAS*, 396, 354
- Grillo, C., Lombardi, M., & Bertin, G. 2008, *A&A*, 477, 397
- Holanda, R. F. L., Lima, J. A. S., & Ribeiro, M. B., 2010, *ApJ*, 722, L233
- Jaroszyński, M., & Kostrzewa-Rutkowska, Z. 2012, *MNRAS*, 424, 325
- Jørgensen, I., Franx, M. & Kjaergard, P. 1995a, *MNRAS*, 273, 1097
- Jørgensen, I., Franx, M. & Kjaergard, P. 1995b, *MNRAS*, 276, 1341
- Jullo, E., et al. 2010, *Science*, 329, 924
- Keeton, C. R., Kochanek, C. S., & Seljak, U. 1997, *ApJ*, 487, 42
- Kochanek, C. S., & Apostolakis, J. 1988, *MNRAS*, 235, 1073
- Kochanek C., et al. 2000, *ApJ*, 543, 131
- Koopmans, L.V.E. & Treu, T. 2002, *ApJ*, 583, 606
- Koopmans L.V.E. 2005, *Proceedings of XXIst IAP Colloquium, “Mass Profiles & Shapes of Cosmological Structures”* (Paris, 4-9 July 2005), eds G. A. Mamon, F. Combes, C. Deffayet, B. Fort (Paris: EDP Sciences) [astro-ph/0511121]
- Koopmans, L.V.E., et al. 2006, *ApJ*, 649, 599
- Koopmans, L.V.E., et al. 2009, *ApJ*, 703, L51
- Lewis, A., & Bridle, S. 2002, *PRD*, 66, 103
- Linder, E. V. 2003, *PRD*, 68, 083503

- Linder, E. V. 2004, PRD, 70, 043534
- Linder, E. V. 2011, PRD, 84, 123529
- Meneghetti, M., et al. 2005, A&A, 442, 413
- Oguri, M., et al. 2012, AJ, 143, 120
- Paczyński, B., & Górski, K. 1981, ApJ, 248, L101
- Perlmutter, S., et al. 1999, ApJ, 517, 565
- Piórkowska A., et al. 2013, Acta Phys. Polon. B, 44, 2397
- Ratnatunga, K. U., Griffiths, R. E., & Ostrander, E. J. 1999, AJ, 117, 2010
- Ratra, B., Peebles, P. E. J., 1988, PRD, 37, 3406
- Refsdal, S. 1964, MNRAS, 128, 295
- Riess, A. G., et al. 1998, AJ, 116, 1009
- Ruff, A., et al. 2011, ApJ, 727, 96
- Rusin, D., Kochanek, C. S., & Keeton, C. R. 2003, ApJ, 595, 29
- Schneider, P., Ehlers, J., & Falco, E. E. 1992, Gravitational Lenses
- Schneider, P. & Sluse, D. 2013, A&A, 559, A37
- Sereno, M. 2002, A&A, 393, 757
- Shu, Y. et al., “The Sloan Lens ACS Survey, XII. Extending Strong Lensing to Lower Masses”, (2014) ApJ submitted [arXiv: 1407.2240]
- Sonnenfeld, A., Gavazzi, R., Suyu, S.H., Treu, T., Marshall, P.J. 2013a, ApJ, 777, 97 [arXiv:1307.4764]
- Sonnenfeld, A., Treu, T., Gavazzi, R., Suyu, S.H., Marshall, P.J., Auger, M.W., Nipoti, C., 2013b, ApJ, 777, 98 [arXiv:1307.4759v1]
- Suyu, S. H, et al. 2010, ApJ, 711, 201
- Suzuki, N., et al. 2012, ApJ, 746, 85
- Treu, T., & Koopmans, L.V.E. 2002, ApJ, 575, 87
- Treu, T., & Koopmans, L.V.E. 2004, ApJ, 611, 739
- Treu, T., et al. 2006, ApJ, 650, 1219

Uzan, J. P., Aghanim, N., & Mellier, Y. 2004, PRD, 70, 083533

Wambsganss, J., Bode, P., & Ostriker, J. P., 2005, ApJ, 635, L1

Table 1. Compilation of strong lensing systems

Name	z_l	z_s	σ_{ap} [km/s]	θ_E ["]	survey	θ_{ap} ["]	θ_{eff} ["]	σ_0 [km/s]
J0151+0049	0.517	1.364	219±39	0.68	BELLS	1	0.89	226±40
J0747+5055	0.438	0.898	328±60	0.75	BELLS	1	1.24	334±61
J0747+4448	0.437	0.897	281±52	0.61	BELLS	1	2.87	277±51
J0801+4727	0.483	1.518	98±24	0.49	BELLS	1	0.57	103±25
J0830+5116	0.53	1.332	268±36	1.14	BELLS	1	1.1	274±37
J0944-0147	0.539	1.179	204±34	0.72	BELLS	1	1.35	207±35
J1159-0007	0.579	1.346	165±41	0.68	BELLS	1	0.99	170±42
J1215+0047	0.642	1.297	262±45	1.37	BELLS	1	1.42	266±46
J1221+3806	0.535	1.284	187±48	0.7	BELLS	1	0.93	193±49
J1234-0241	0.49	1.016	122±31	0.53	BELLS	1	1.61	123±31
J1318-0104	0.659	1.396	177±27	0.68	BELLS	1	1.06	182±28
J1337+3620	0.564	1.182	225±35	1.39	BELLS	1	1.6	227±35
J1349+3612	0.44	0.893	178±18	0.75	BELLS	1	2.03	178±18
J1352+3216	0.463	1.034	161±21	1.82	BELLS	1	1.35	164±21
J1522+2910	0.555	1.311	166±27	0.74	BELLS	1	1.08	170±28
J1541+1812	0.56	1.113	174±24	0.64	BELLS	1	0.59	183±25
J1542+1629	0.352	1.023	210±16	1.04	BELLS	1	1.45	213±16
J1545+2748	0.522	1.289	250±37	1.21	BELLS	1	2.65	247±37
J1601+2138	0.544	1.446	207±36	0.86	BELLS	1	0.63	217±38
J1611+1705	0.477	1.211	109±23	0.58	BELLS	1	1.33	111±23
J1631+1854	0.408	1.086	272±14	1.63	BELLS	1	2.07	272±14
J1637+1439	0.391	0.874	208±30	0.65	BELLS	1	0.89	215±31
J2122+0409	0.626	1.452	324±56	1.58	BELLS	1	1.76	326±56
J2125+0411	0.363	0.978	247±17	1.2	BELLS	1	1.47	250±17
J2303+0037	0.458	0.936	274±31	1.02	BELLS	1	1.35	278±31
J0008-0004	0.44	1.192	193±36	1.16	SLACS	1.5	1.71	197±37
J0029-0055	0.227	0.931	229±18	0.96	SLACS	1.5	2.16	232±18
J0037-0942	0.196	0.632	279±10	1.53	SLACS	1.5	2.19	283±10
J0044+0113	0.12	0.196	266±13	0.79	SLACS	1.5	2.61	267±13
J0109+1500	0.294	0.525	251±19	0.69	SLACS	1.5	1.38	259±20
J0157-0056	0.513	0.924	295±47	0.79	SLACS	1.5	1.06	308±49
J0216-0813	0.332	0.524	333±23	1.16	SLACS	1.5	2.67	335±23
J0252+0039	0.28	0.982	164±12	1.04	SLACS	1.5	1.39	169±12

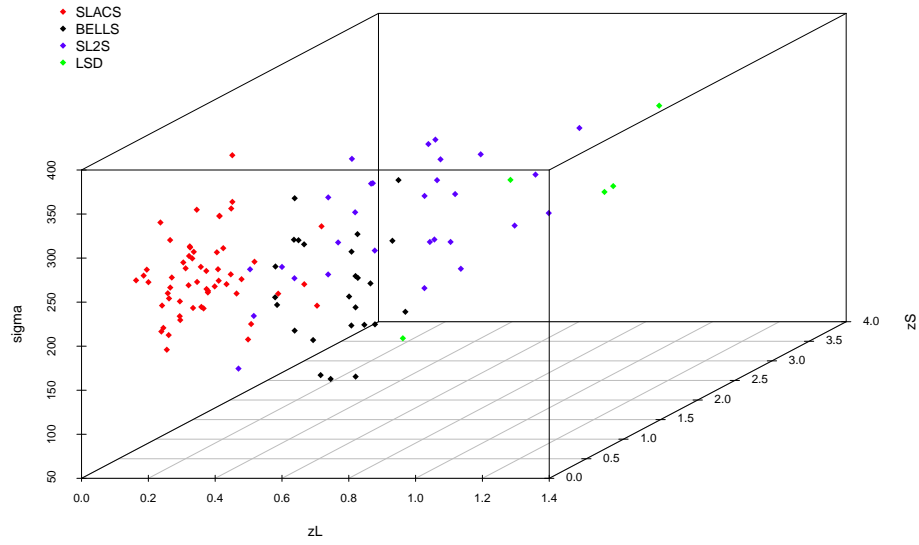


Fig. 1.— Scatter plot of our sample of 118 strong lensing systems. One can see a fair coverage of redshifts in the combined sample.

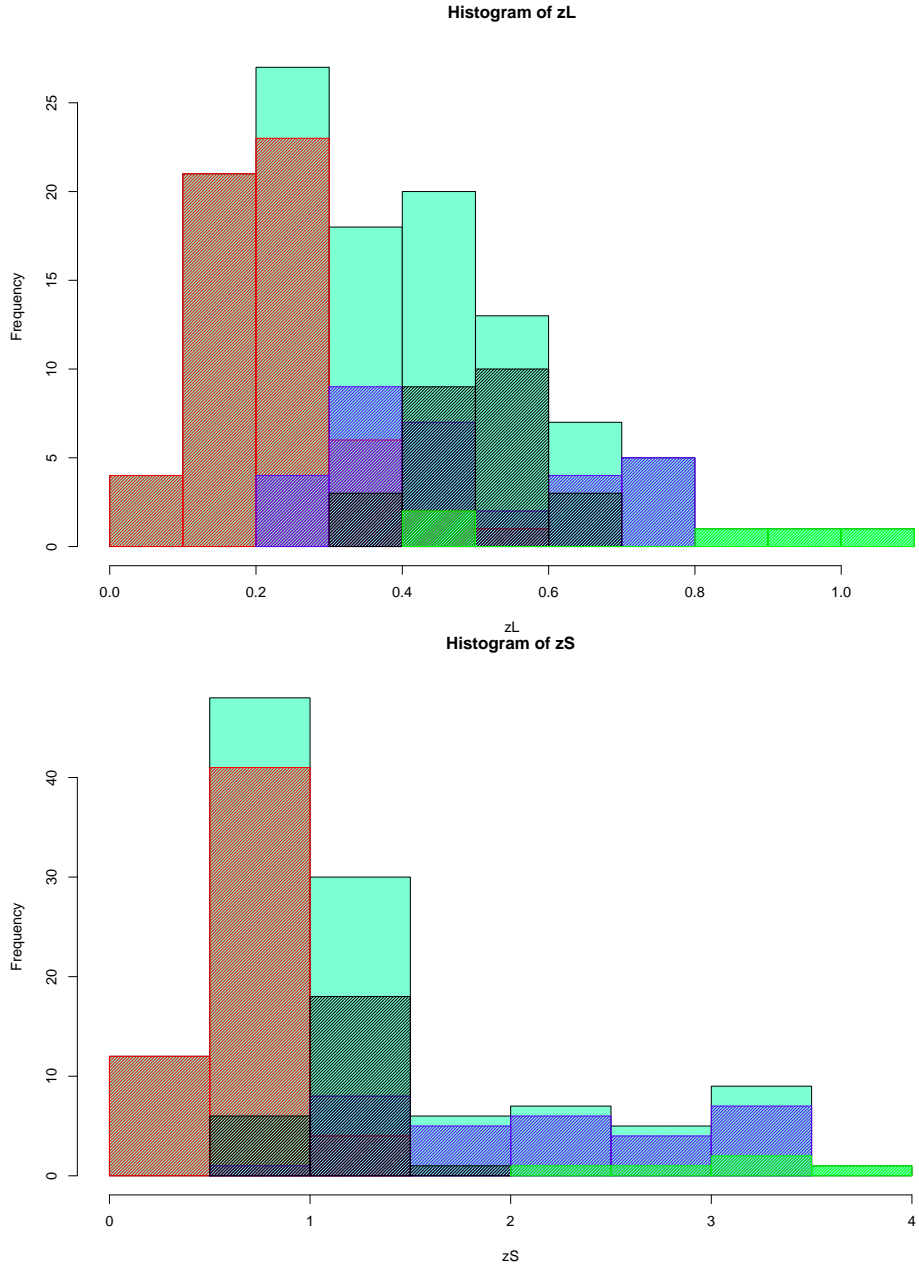


Fig. 2.— Histogram of lens (upper panel) and source redshifts (lower panel). Different colors show contribution of different surveys superimposed on the overall histogram. The color convention is the same as for Fig. 1.

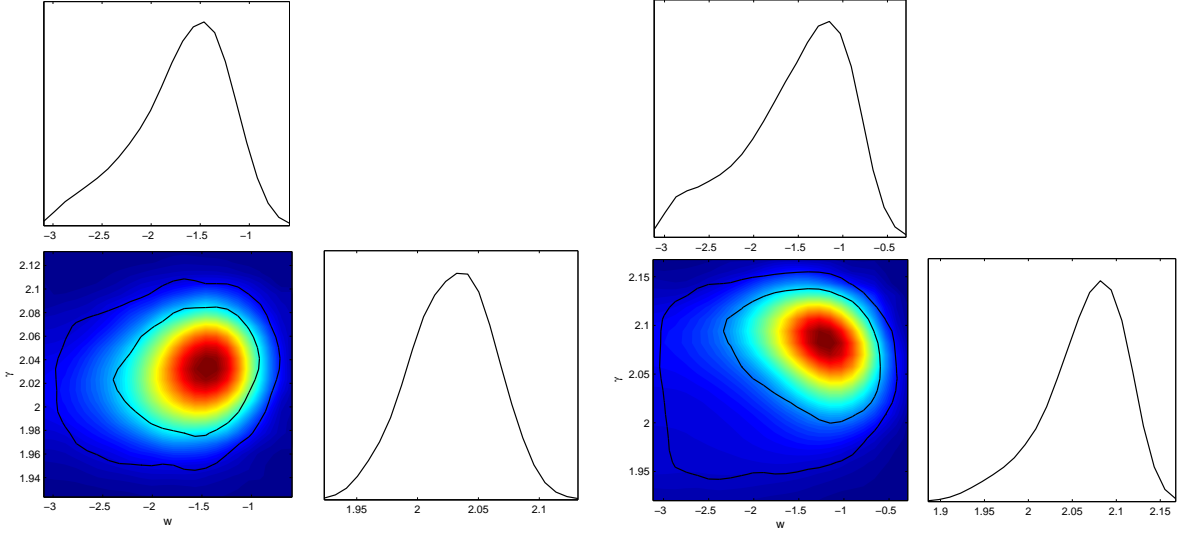


Fig. 3.— Joint fits of mass density slope γ and w coefficient in the XCDM model. Left panel shows the results obtained with velocity dispersion within the aperture σ_{ap} while on the right panel corrected velocity dispersion σ_0 was used. $\Omega_m = 0.315$ is assumed based on the Planck observations (Ade et al. 2014). Marginalized probability density functions for γ and w are also shown.

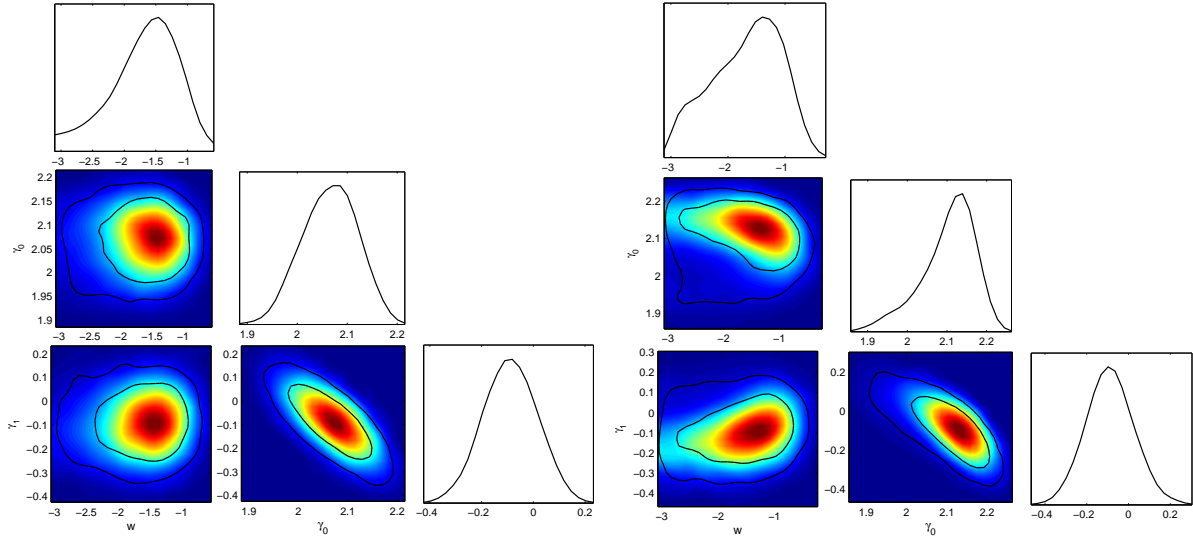


Fig. 4.— Joint fits of w coefficient in the XCDM model and mass density slope parameters (γ_0 , γ_1) in evolving slope scenario $\gamma(z) = \gamma_0 + \gamma_1 z_l$. Left and right panels display the results obtained by using σ_{ap} and σ_0 respectively.

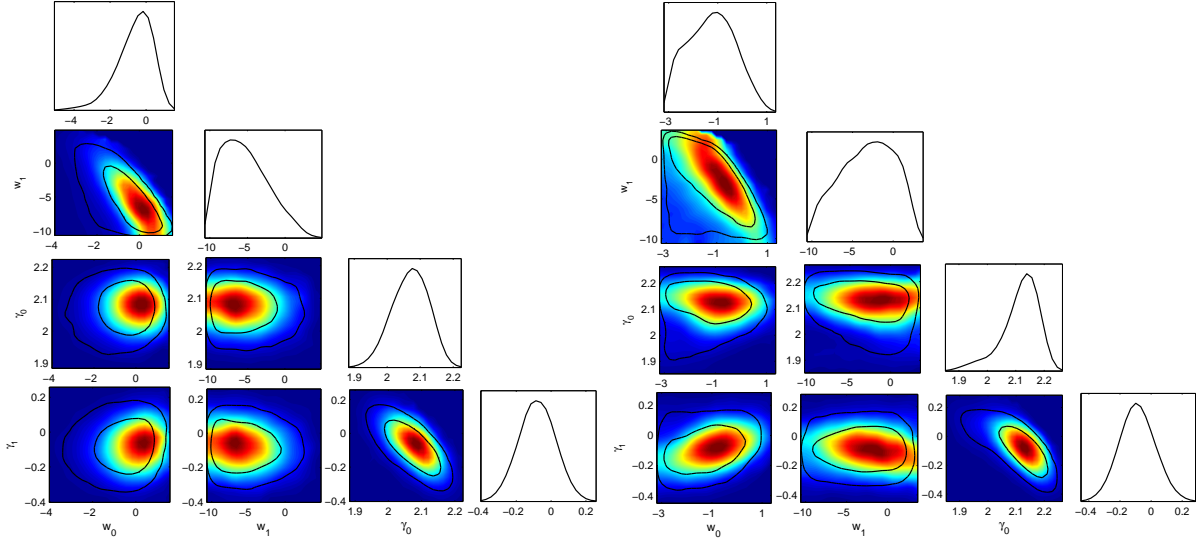


Fig. 5.— Joint fits of (w_0, w_1) evolving cosmic equation of state coefficients in the CPL parametrization. Lensing galaxies were assumed to have evolving mass density slope $\gamma(z) = \gamma_0 + \gamma_1 z_l$ and (γ_0, γ_1) parameters. Left and right panels display the results obtained by using σ_{ap} and σ_0 respectively.

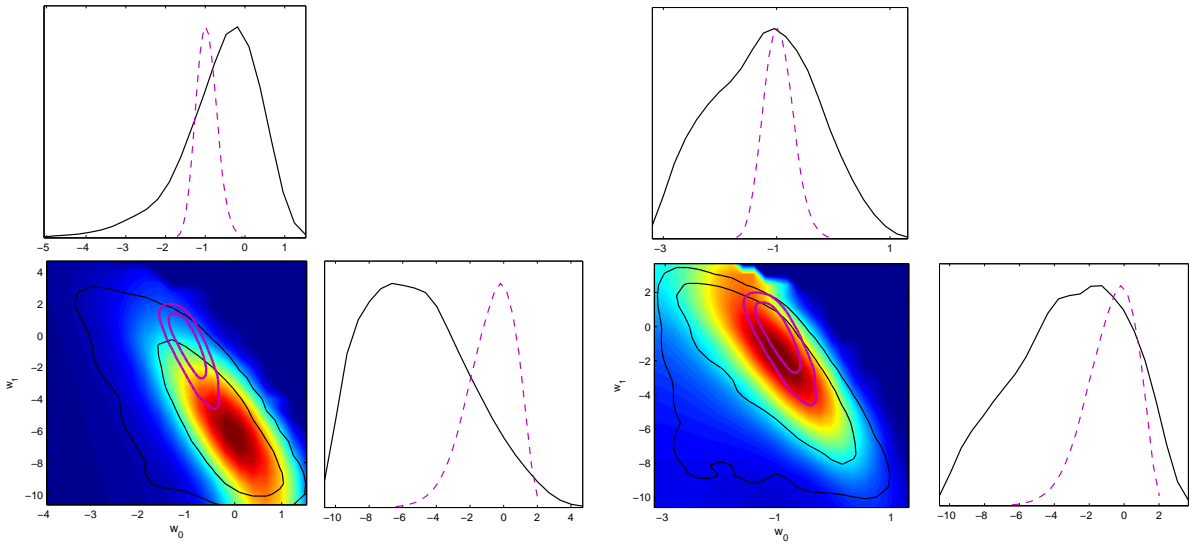


Fig. 6.— Joint fits of (w_0, w_1) evolving cosmic equation of state coefficients in the CPL parametrization. Lensing galaxies were assumed to have evolving mass density slope $\gamma(z) = \gamma_0 + \gamma_1 z_l$ and (γ_0, γ_1) parameters were fixed at our best-fit values in Λ CDM model. Left and right panels display the results obtained by using σ_{ap} and σ_0 respectively.

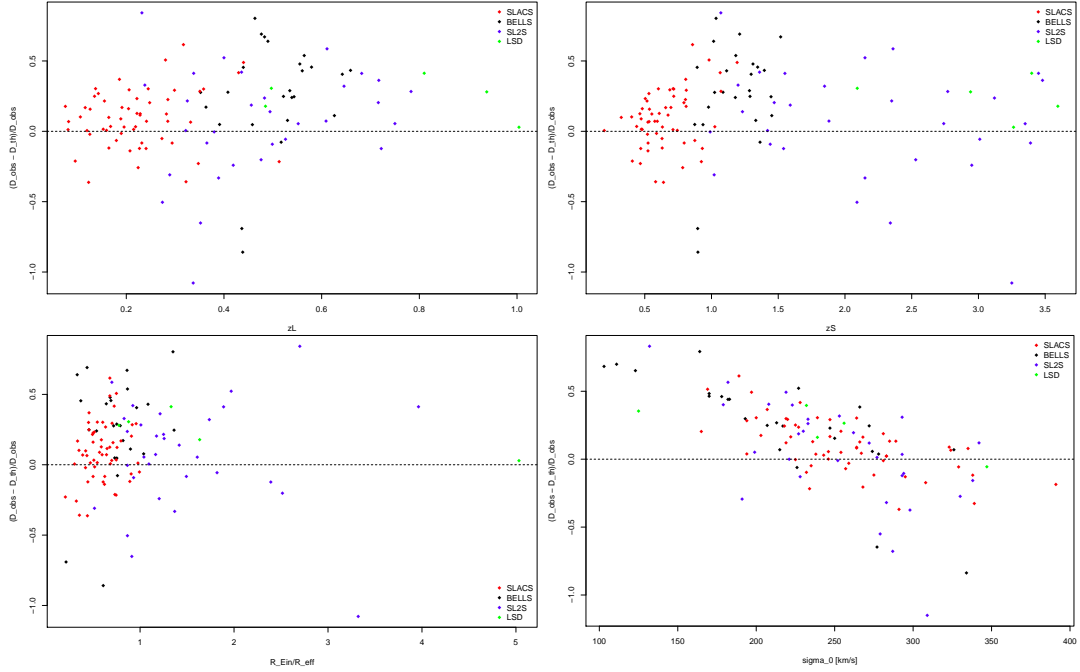


Fig. 7.— Relative residuals in our observable: $(\mathcal{D}^{obs} - \mathcal{D}^{th})/\mathcal{D}^{obs}$ as a function of lens redshift z_l , source redshift z_s , Einstein radius relative to the effective radius R_E/R_{eff} and the aperture corrected velocity dispersion σ_0 .

Table 1—Continued

Name	z_l	z_s	σ_{ap} [km/s]	θ_E ["]	survey	θ_{ap} ["]	θ_{eff} ["]	σ_0 [km/s]
J0330-0020	0.351	1.071	212±21	1.1	SLACS	1.5	1.2	220±22
J0405-0455	0.075	0.81	160±8	0.8	SLACS	1.5	1.36	165±8
J0728+3835	0.206	0.688	214±11	1.25	SLACS	1.5	1.78	219±11
J0737+3216	0.322	0.581	338±17	1	SLACS	1.5	2.82	339±17
J0808+4706	0.219	1.025	236±11	1.23	SLACS	1.5	2.42	238±11
J0822+2652	0.241	0.594	259±15	1.17	SLACS	1.5	1.82	264±15
J0841+3824	0.116	0.657	225±11	1.41	SLACS	1.5	4.21	222±11
J0903+4116	0.43	1.065	223±27	1.29	SLACS	1.5	1.78	228±28
J0912+0029	0.164	0.324	326±12	1.63	SLACS	1.5	3.87	323±12
J0935-0003	0.348	0.467	396±35	0.87	SLACS	1.5	4.24	391±35
J0936+0913	0.19	0.588	243±12	1.09	SLACS	1.5	2.11	246±12
J0946+1006	0.222	0.608	263±21	1.38	SLACS	1.5	2.35	266±21
J0956+5100	0.24	0.47	334±17	1.33	SLACS	1.5	2.19	338±17
J0959+0410	0.126	0.535	197±13	0.99	SLACS	1.5	1.39	203±13
J1016+3859	0.168	0.439	247±13	1.09	SLACS	1.5	1.46	254±13
J1020+1122	0.282	0.553	282±18	1.2	SLACS	1.5	1.59	289±18
J1023+4230	0.191	0.696	242±15	1.41	SLACS	1.5	1.77	247±15
J1100+5329	0.317	0.858	187±23	1.52	SLACS	1.5	2.24	189±23
J1106+5228	0.096	0.407	262±13	1.23	SLACS	1.5	1.68	268±13
J1112+0826	0.273	0.63	320±20	1.49	SLACS	1.5	1.5	329±21
J1134+6027	0.153	0.474	239±12	1.1	SLACS	1.5	2.02	243±12
J1142+1001	0.222	0.504	221±22	0.98	SLACS	1.5	1.91	225±22
J1143-0144	0.106	0.402	269±13	1.68	SLACS	1.5	4.8	264±13
J1153+4612	0.18	0.875	226±15	1.05	SLACS	1.5	1.16	235±16
J1204+0358	0.164	0.631	267±17	1.31	SLACS	1.5	1.47	275±17
J1205+4910	0.215	0.481	281±14	1.22	SLACS	1.5	2.59	283±14
J1213+6708	0.123	0.64	292±15	1.42	SLACS	1.5	3.23	291±15
J1218+0830	0.135	0.717	219±11	1.45	SLACS	1.5	3.18	218±11
J1250+0523	0.232	0.795	252±14	1.13	SLACS	1.5	1.81	257±14
J1251-0208	0.224	0.784	233±23	0.84	SLACS	1.5	2.61	234±23
J1330-0148	0.081	0.712	185±9	0.87	SLACS	1.5	0.89	194±9
J1402+6321	0.205	0.481	267±17	1.35	SLACS	1.5	2.7	268±17
J1403+0006	0.189	0.473	213±17	0.83	SLACS	1.5	1.46	219±17

Table 1—Continued

Name	z_l	z_s	σ_{ap} [km/s]	θ_E ["]	survey	θ_{ap} ["]	θ_{eff} ["]	σ_0 [km/s]
J1416+5136	0.299	0.811	240±25	1.37	SLACS	1.5	1.43	247±26
J1430+4105	0.285	0.575	322±32	1.52	SLACS	1.5	2.55	324±32
J1436-0000	0.285	0.805	224±17	1.12	SLACS	1.5	2.24	227±17
J1451-0239	0.125	0.52	223±14	1.04	SLACS	1.5	2.48	225±14
J1525+3327	0.358	0.717	264±26	1.31	SLACS	1.5	2.9	264±26
J1531-0105	0.16	0.744	279±14	1.71	SLACS	1.5	2.5	281±14
J1538+5817	0.143	0.531	189±12	1	SLACS	1.5	1.58	194±12
J1621+3931	0.245	0.602	236±20	1.29	SLACS	1.5	2.14	239±20
J1627-0053	0.208	0.524	290±14	1.23	SLACS	1.5	1.98	295±14
J1630+4520	0.248	0.793	276±16	1.78	SLACS	1.5	1.96	281±16
J1636+4707	0.228	0.674	231±15	1.09	SLACS	1.5	1.68	236±15
J2238-0754	0.137	0.713	198±11	1.27	SLACS	1.5	2.33	200±11
J2300+0022	0.228	0.464	279±17	1.24	SLACS	1.5	1.83	285±17
J2303+1422	0.155	0.517	255±16	1.62	SLACS	1.5	3.28	254±16
J2321-0939	0.082	0.532	249±8	1.6	SLACS	1.5	4.11	246±8
J2341+0000	0.186	0.807	207±13	1.44	SLACS	1.5	3.15	207±13
Q0047-2808	0.485	3.595	229±15	1.34	LSD	1.25	0.82	239±16
CFRS03-1077	0.938	2.941	251±19	1.24	LSD	1.25	1.6	256±19
HST14176	0.81	3.399	224±15	1.41	LSD	1.25	1.06	232±16
HST15433	0.497	2.092	116±10	0.36	LSD	1.25	0.41	125±11
MG2016	1.004	3.263	328±32	1.56	LSD	0.65	0.31	347±34
J0212-0555	0.75	2.74	273±22	1.27	SL2S	0.9	1.22	277±22
J0213-0743	0.717	3.48	293±34	2.39	SL2S	1	1.97	293±34
J0214-0405	0.609	1.88	287±47	1.41	SL2S	1	1.21	293±48
J0217-0513	0.646	1.847	239±27	1.27	SL2S	1.5	0.73	253±29
J0219-0829	0.389	2.15	289±23	1.3	SL2S	1	0.95	298±24
J0223-0534	0.499	1.44	288±28	1.22	SL2S	1	1.31	293±28
J0225-0454	0.238	1.199	234±21	1.76	SL2S	1	2.12	233±21
J0226-0420	0.494	1.232	263±24	1.19	SL2S	1	0.84	272±25
J0232-0408	0.352	2.34	281±26	1.04	SL2S	1	1.14	287±27
J0848-0351	0.682	1.55	197±21	0.85	SL2S	0.9	0.45	208±22
J0849-0412	0.722	1.54	320±24	1.1	SL2S	0.9	0.46	338±25
J0849-0251	0.274	2.09	276±35	1.16	SL2S	0.9	1.34	279±35

Table 1—Continued

Name	z_l	z_s	σ_{ap} [km/s]	θ_E ["]	survey	θ_{ap} ["]	θ_{eff} ["]	σ_0 [km/s]
J0850-0347	0.337	3.25	290±24	0.93	SL2S	0.7	0.28	309±26
J0855-0147	0.365	3.39	222±25	1.03	SL2S	0.7	0.69	228±26
J0855-0409	0.419	2.95	281±22	1.36	SL2S	0.7	1.13	283±22
J0904-0059	0.611	2.36	183±21	1.4	SL2S	0.9	2	182±21
J0959+0206	0.552	3.35	188±22	0.74	SL2S	0.9	0.46	199±23
J1359+5535	0.783	2.77	228±29	1.14	SL2S	1	1.13	233±30
J1404+5200	0.456	1.59	342±20	2.55	SL2S	1	2.03	342±20
J1405+5243	0.526	3.01	284±21	1.51	SL2S	1	0.83	294±22
J1406+5226	0.716	1.47	253±19	0.94	SL2S	1	0.8	262±20
J1411+5651	0.322	1.42	214±23	0.93	SL2S	1	0.85	221±24
J1420+5258	0.38	0.99	246±23	0.96	SL2S	1	1.11	252±24
J1420+5630	0.483	3.12	228±19	1.4	SL2S	1	1.62	230±19
J2203+0205	0.4	2.15	213±21	1.95	SL2S	1	0.99	219±22
J2205+0147	0.476	2.53	317±30	1.66	SL2S	0.9	0.66	330±31
J2213-0009	0.338	3.45	165±20	1.07	SL2S	1	0.27	179±22
J2219-0017	0.289	1.02	189±20	0.52	SL2S	0.7	1.01	191±20
J2220+0106	0.232	1.07	127±15	2.16	SL2S	1	0.8	132±16
J2221+0115	0.325	2.35	222±23	1.4	SL2S	1	1.12	227±24
J2222+0012	0.436	1.36	221±22	1.44	SL2S	1	1.56	223±22

Table 2. Dark energy (Λ CDM model and CPL parametrization) constraints obtained on the full 118 strong lensing (SL) sample.

Cosmology (Sample)	w_0	w_1	γ_0	γ_1
XCDM1 (SL; σ_{ap})	$w_0 = -1.45^{+0.54}_{-0.95}$	$w_1 = 0$	$\gamma_0 = 2.03 \pm 0.06$	$\gamma_1 = 0$
XCDM1 (SL; σ_0)	$w_0 = -1.15^{+0.56}_{-1.20}$	$w_1 = 0$	$\gamma_0 = 2.07 \pm 0.07$	$\gamma_1 = 0$
XCDM2 (SL; σ_{ap})	$w_0 = -1.48^{+0.54}_{-0.94}$	$w_1 = 0$	$\gamma_0 = 2.06 \pm 0.09$	$\gamma_1 = -0.09 \pm 0.16$
XCDM2 (SL; σ_0)	$w_0 = -1.35^{+0.67}_{-1.50}$	$w_1 = 0$	$\gamma_0 = 2.13^{+0.07}_{-0.12}$	$\gamma_1 = -0.09 \pm 0.17$
CPL1 (SL; σ_{ap})	$w_0 = -0.15^{+1.27}_{-1.60}$	$w_1 = -6.95^{+7.25}_{-3.05}$	$\gamma_0 = 2.08 \pm 0.09$	$\gamma_1 = -0.09 \pm 0.17$
CPL1 (SL; σ_0)	$w_0 = -1.00^{+1.54}_{-1.95}$	$w_1 = -1.85^{+4.85}_{-6.75}$	$\gamma_0 = 2.14^{+0.07}_{-0.10}$	$\gamma_1 = -0.10 \pm 0.18$
CPL2 (SL; σ_{ap})	$w_0 = -0.16^{+1.21}_{-1.48}$	$w_1 = -6.25^{+6.25}_{-3.75}$	$\gamma_0 = 2.08$	$\gamma_1 = -0.09$
CPL2 (SL; σ_0)	$w_0 = -1.05^{+1.43}_{-1.77}$	$w_1 = -1.65^{+4.25}_{-6.35}$	$\gamma_0 = 2.14$	$\gamma_1 = -0.10$
CPL2 (SN)	$w_0 = -1.00 \pm 0.40$	$w_1 = -0.12^{+1.58}_{-2.78}$	\square	\square

^aIn our fits we separately considered observed velocity dispersions σ_{ap} and corrected velocity dispersions σ_0 , Λ CDM1 corresponds to assumption of non-evolving power-law index γ , while Λ CDM2 assumes its evolution $\gamma(z) = \gamma_0 + \gamma_1 z$. Fixed prior of $\Omega_m = 0.315$ was assumed according to the Planck data. While fitting CPL parameters we assumed evolving lens mass density with γ_0 and γ_1 as free parameters (CPL1) and then fixed them at best-fit values (CPL2). For comparison fits of CPL parameters using Union2.1 supernovae data (SN) is shown.